



# Influence of gas phase and surface reactions on plasma polymerization

Sébastien Guimond, Urs Schütz, Barbara Hanselmann, Enrico Körner, Dirk Hegemann \*

Empa, Swiss Federal Laboratories for Materials Science and Technology, Lerchenfeldstrasse 5, 9014 St. Gallen, Switzerland

## ARTICLE INFO

Available online 29 March 2011

**Keywords:**  
RF plasma  
Deposition rate  
a-C:H:N  
Ion bombardment  
Functional groups

## ABSTRACT

The formation of plasma polymers is based on multistep reactions that are taking place both in the gas phase and on the surface of the growing film. In order to gain more insights and to control plasma polymerization processes, some assumptions can be made that allow a macroscopic description. Following this idea, a concept was developed based on the energy input both into the gas phase (plasma) and during film growth (surface) that helps in up-scaling plasma polymerization processes. In order to test this concept, various a-C:H:N thin films were deposited under different  $\text{NH}_3/\text{C}_2\text{H}_4$  gas ratios, power inputs  $W$ , and gas flow rates  $F$ . Thereby, the energy consumed in the gas phase is controlled by  $W/F$  yielding a flux of film-forming species. The comparison of two comparable plasma reactors of different sizes indicate that while the reaction parameter  $W/F$  plays a major role for the transfer of plasma polymerization processes, the energy input into the film by ion bombardment during film growth should also be taken into account.

© 2011 Elsevier B.V. All rights reserved.

## 1. Introduction

The deposition of functional plasma polymer thin films enables the adjustment of surface properties for different applications such as hydrophilic textiles with improved sweat management or cytocompatible materials for tissue engineering [1–3]. Industrial applications require reliable and manageable processes, which can be transferred to production-scale reactors [4]. This often has a strong influence on the choice of process gasses and reactor geometry, for instance. Moreover, plasma polymers optimized with respect to functionality and stability in aqueous environments are often required [5]. Due to the enormous difficulties lying in the microscopic description of plasma polymerization processes, we are considering a macroscopic approach which is based on the energy input into the plasma process [6–8]. Since plasma polymerization processes involve both gas phase reactions and surface reactions, it is important to consider the energy input into the plasma zone as well as the energy input into the film itself. While the former gives the energy invested per particle within the active plasma zone, the latter is mostly related to ion bombardment at the growing film surface. Both reaction parameters are mainly determined by the external parameters power input  $W$  and unit of gas flow  $F$  when some internal parameters such as power absorption, direction of gas flow, plasma expansion, plasma density, and sheath potential are known.

Assuming that the film growth is limited by the activation of the monomer in the gas phase (reaction kinetics limited regime), i.e. it is

not determined by diffusive transport or high overall conversion, a quasi-Arrhenius relation can be used to describe the mass deposition rate per unit of gas (monomer) flow  $R_m/F$  as a function of the specific energy input  $W/F$  as reaction parameter:

$$\frac{R_m}{F} = G \exp\left(-\frac{E_a}{W/F}\right), \quad (1)$$

where  $E_a$  represents an apparent activation energy (activation barrier) and  $G$  is a reactor and process dependent factor related to the maximum monomer conversion into film growth [9–12].

The energy dissipated in the film during growth, on the other hand, is approximated by the energy density  $\varepsilon$  (in  $\text{eV nm}^{-3}$ ):

$$\varepsilon = \frac{\Gamma_i E_{\text{mean}}}{R}, \quad (2)$$

which represents ion bombardment (ion flux times mean ion energy) per film growth rate  $R$  (in  $\text{nm s}^{-1}$ ) [13]. The ion flux  $\Gamma_i$  incident on the substrate (in  $\text{nm}^{-2} \text{s}^{-1}$ ) can be estimated using a model proposed by Lieberman et al. [14]:

$$\Gamma_i = n_0 v_B \cos \theta \quad (3)$$

with  $n_0$  being the plasma density in the plasma bulk (which equals the electron density  $n_e$  for electropositive gasses) and  $v_B$ , the Bohm velocity of the ions entering the plasma sheath. The reduction of the number of ions fulfilling the Bohm criteria due to collisions is considered by the factor  $\cos \theta$  which in turn depends on the plasma length and the ion mean free path – it is roughly 0.2 for the plasma conditions considered here (pressure of 10 Pa). The mean energy

\* Corresponding author. Tel.: +41 587657268; fax: +41 587657569.  
E-mail address: [dirk.hegemann@empa.ch](mailto:dirk.hegemann@empa.ch) (D. Hegemann).

$E_{mean}$  of the ions impinging on the substrate (in [eV]) can be estimated from the sheath potential  $V_s$  according to a study by Manenschijn and Goedher [15]:

$$E_{mean} = eV_s \cos \varphi, \quad (4)$$

where the factor  $\cos \varphi$  regards collisions in the plasma sheath and depends on the sheath length, the ion mean free path and the type of collisions (elastic or charge-exchange). For the considered plasma conditions (pressure of 10 Pa) it is roughly 0.15. The sheath voltage is proportional to the excitation voltage with  $V_s = 0.39 V_0$  for symmetric RF discharges [14]. Hence, measuring the electron density and the excitation voltage (which both depend on power input  $W$ , but not on flow rate  $F$ ) as well as the deposition rate enables the calculation of the energy density according to Eqs. (2)–(4).

A macroscopic approach has thus been used in this work to investigate plasma polymerization processes for the deposition of amine-functional a-C:H:N coatings that can also be transferred to industrial reactors [8,16].

## 2. Experimental

Two different reactors were used to investigate the transfer of plasma polymerization processes: a lab-scale batch reactor and a pilot-scale web coater (Fig. 1). The (symmetric) batch reactor is composed of two plane parallel electrodes of the same size (30 cm in diameter) separated by a glass cylinder [16]. The distance between the upper showerhead electrode and the lower RF-driven (13.56 MHz) electrode was 5 cm. The pressure was fixed at 10 Pa, while the power input was varied between 7 and 150 W. The monomer flow rate of ethylene ( $C_2H_4$ ) was held constant at 8 sccm. Beside pure  $C_2H_4$  discharges, ammonia ( $NH_3$ ) was added with 8 and 16 sccm to obtain gas ratios of  $NH_3/C_2H_4$  of 1:1 and 2:1. The web coater consisted of a RF-driven (13.56 MHz) drum electrode (with a diameter of 59 cm and a length of 65 cm) enclosed in a larger cylindrical vessel [17,18]. The substrates were fixed on the drum which was rotated during plasma deposition. The gas inlet was distributed at four positions (showerhead) around the drum to obtain a homogeneous gas flow. The power input was varied between 300 and 1000 W at a pressure of 10 Pa. The following gas flow rates were used: 100 sccm  $C_2H_4$  (pure  $C_2H_4$  discharge), 250 sccm  $C_2H_4$  with 250 sccm  $NH_3$  ( $NH_3/C_2H_4 = 1:1$ ), and 100 sccm  $C_2H_4$  with 250 sccm  $NH_3$  ( $NH_3/C_2H_4 = 2.5:1$ ). Due to the (nearly) symmetric set-up of the electrodes in both reactors, the bias voltage remained small and the discharge homogeneously occupied the whole inter-electrode space allowing for the comparison of both reactors.

The deposited mass was measured by weighing thin glass slide substrates right before and after deposition, while profilometry was used to determine the film thickness. The film density was simply calculated from both values. A V/I probe (ENI Model 1065) was used to measure excitation voltage  $V_0$  and absorbed power  $W$  (the latter had a value around 80% of the generator's nominal power). Electron densities were measured within the batch reactor using microwave

interferometry (JE PlasmaConsult MWI 2650) by integrating over the line of sight with a plasma length of 28 cm (see Fig. 1). The method is based on the phase shift of 26.5 GHz microwave radiation transmitted through the plasma [19]. Fig. 2 displays the obtained electron densities, which show a linear dependence over a broad range of power input, thus showing reliable plasma conditions. Since the electron density could not easily be measured for the web coater (due to technical reasons), we did a comparison based on the power input per plasma volume, the latter being roughly  $66,000 \text{ cm}^3$  for the web coater and  $1850 \text{ cm}^3$  for the batch reactor. XPS surface analysis was performed in a PHI 5600 LS system, using a non-monochromatized  $MgK\alpha$  source and an electron take-off angle of  $45^\circ$ . All samples were analyzed within one day following their deposition. The surface concentration of primary amines,  $[-NH_2]$ , was determined by XPS after derivatization with 4-(trifluoromethyl)benzaldehyde (TFBA) vapor [20].

## 3. Results and discussion

We have recently investigated the plasma polymer growth from  $CO_2/C_2H_4$  discharges with varying gas ratio and flow rates [7,11]. We found that the evolution of the deposition rate as a function of the reaction parameter  $W/F$  follows an Arrhenius-like behavior according to Eq. (1) over a broad parameter range. This range was named regime II (reaction kinetics limited range), while regime I shows deviations from the Arrhenius-like behavior at low energy input and regime III is indicated by deviations at the high energy side [7]. Similar results were obtained for  $NH_3/C_2H_4$  discharges as shown in Fig. 3 and as already reported in the literature [21–23]. While examining a broad range of  $W/F$  within the batch reactor, the three regimes including the linear Arrhenius-like regime can clearly be seen for the  $NH_3/C_2H_4$  gas ratio of 1:1. With increasing gas ratio, the deposition rates were found to be reduced compared to pure  $C_2H_4$  discharges, which is ascribed to formation of CN and HCN species in the gas phase yielding incorporation of nitrogen as well as chemical etching during film growth. Nevertheless, the deposition of the a-C:H:N coatings is mainly described by an Arrhenius-like behavior (regime II). Therefore, we assume a similar reaction pathway over a broad range of energy input, where mainly the number of film-forming species is increased. The chemical reaction pathway might proceed via film-forming species which show a high sticking coefficient, but a low to moderate reactivity in the gas phase [24]. Thus, specific reaction channels might be promoted despite of unselective plasma-chemical processes in the gas phase. Moreover, the surface elemental composition of the a-C:H:N plasma polymers was found to be approximately constant within this regime, e.g.  $N/C = 0.24 \pm 0.02$  for  $NH_3/C_2H_4 = 1$  (agreeing well with data obtained by others [25]), while the N content is reduced for regime III.

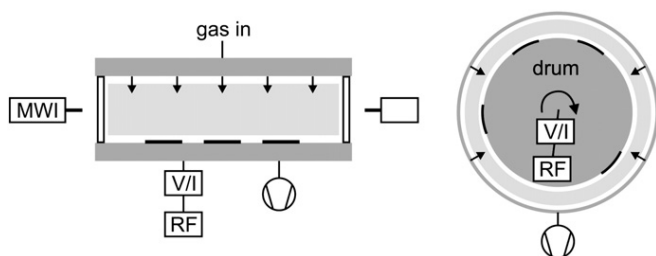


Fig. 1. Scheme of the batch reactor (left) and the web coater (right) experimental set-ups. Substrates were placed on the driven electrode in both cases.

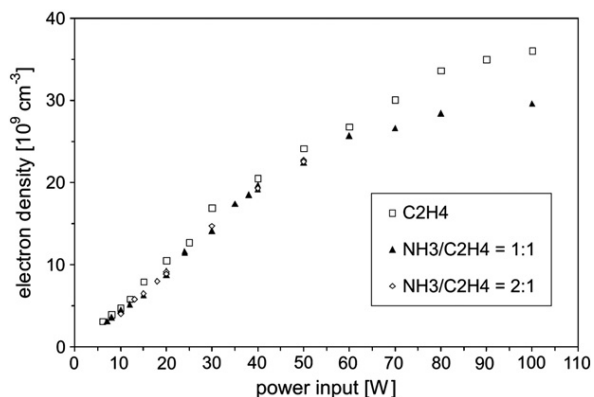


Fig. 2. Electron density measured as a function of power input for the batch reactor.

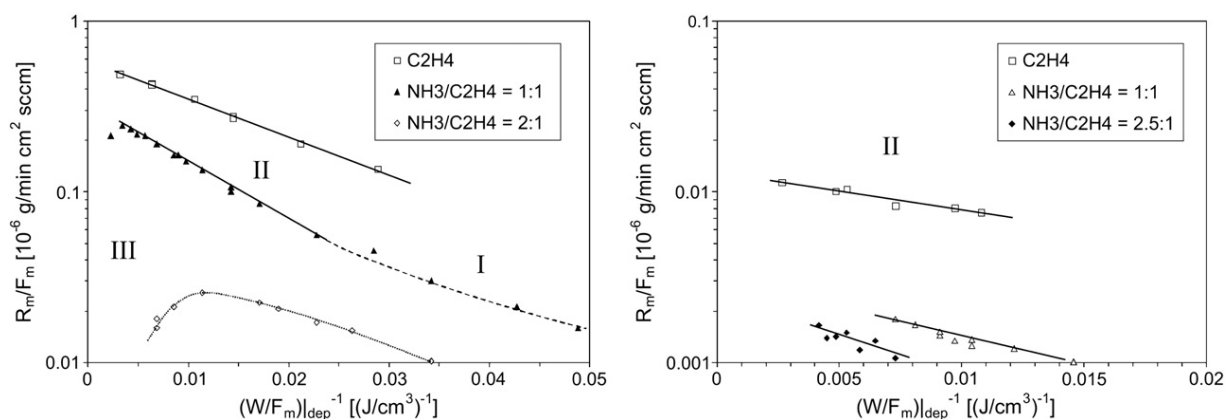


Fig. 3. Arrhenius-like plots of the deposited mass vs. the inverse energy input for  $\text{NH}_3/\text{C}_2\text{H}_4$  and  $\text{C}_2\text{H}_4$  discharges as obtained in the batch reactor (left) and the web coater (right). The different regimes are indicated by roman numbers.

The plasma polymerization performed in the web coater showed very similar results regarding regime II (Fig. 3). Corrected for the actual energy input into the plasma volume, the same slopes of the Arrhenius fits were obtained in both reactors for  $\text{C}_2\text{H}_4$  and  $\text{NH}_3/\text{C}_2\text{H}_4 = 1:1$  ( $51 \text{ J cm}^{-3}$  or  $12 \text{ eV}$  per particle and  $75 \text{ J cm}^{-3}$  or  $18 \text{ eV}$  per particle, respectively) [26]. Note that for the curve of  $\text{NH}_3/\text{C}_2\text{H}_4 = 1$  in the web coater a higher monomer flow (250 sccm as compared to the pure  $\text{C}_2\text{H}_4$  discharge with 100 sccm) was used, resulting in lower  $R_m/F_m$  values. This is attributed to the fact that the absolute deposition rates are also limited by surface reactions (e.g. formation of nucleation sites and incorporation of incoming film-forming species) [11].

For higher  $\text{NH}_3/\text{C}_2\text{H}_4$  gas ratios, however, a different evolution of the deposition rate can be observed between the two reactors. While the web coater data for  $\text{NH}_3/\text{C}_2\text{H}_4 = 2.5:1$  still follow Eq. (1) (with  $E_a = 112 \text{ J cm}^{-3}$  or  $26 \text{ eV}$ ), a flattened curve appeared for  $\text{NH}_3/\text{C}_2\text{H}_4 = 2:1$  in the case of the batch reactor. A similar behavior was already observed for higher  $\text{NH}_3/\text{C}_2\text{H}_2$  gas ratios in the web coater and for a  $\text{CO}_2/\text{C}_2\text{H}_4$  gas ratio of 6:1 in the symmetric batch reactor [11,21]. We ascribed this effect to a stronger influence of ion bombardment in the batch reactor. In order to verify this assumption, we calculated the energy density  $\varepsilon$  during deposition according to Eq. (2) by measuring excitation and bias voltage as well as electron densities assuming electropositive plasmas.

For the batch reactor and  $\text{NH}_3/\text{C}_2\text{H}_4 = 1$ , we obtained values of  $\varepsilon$  around  $1000 \text{ eV nm}^{-3}$  (corresponding to  $\sim 15 \text{ eV}$  per deposited C or N atom) yielding crosslinking and densification of the films, whereas a deviation from the Arrhenius curve appeared at  $\varepsilon > 2000 \text{ eV nm}^{-3}$  (for  $(W/F)^{-1}$  values below  $0.003 (\text{J/cm}^3)^{-1}$ , see Fig. 3). For the higher

$\text{NH}_3/\text{C}_2\text{H}_4$  gas ratio of 2:1, the energy density was constantly above this value, thus supporting the view of ion-induced etching effects. This also explains the increasing film density for higher  $\text{NH}_3/\text{C}_2\text{H}_4$  gas ratios as reported in Ref. [1]. We note here that the density of the films scales more or less linearly over a broad range of  $\log \varepsilon$  (Fig. 4).

Since we could not measure the electron density within the web coater, we assumed in a first approach to have the same values as in the smaller batch reactor when comparing power input per plasma volume yielding comparable excitation voltages  $V_0$  for both reactors. Note that our macroscopic approach to examine the plasma chemical gas phase processes also enables the comparison of different plasma reactors based on the energy input  $(W/F)$  per plasma volume (active plasma zone). However, the obtained values did not match with the measured film densities for both reactors as indicated by the surrounded small dots in Fig. 4. A satisfying match can only be obtained if we assume that the electron densities are actually lower in the web coater, which indicates the importance of plasma reactor geometry (even though the voltage drop through the plasma sheath was comparable for both reactors, i.e. around 100–200 V). A good match could be obtained assuming a four times lower plasma density in the web coater, as shown in Fig. 4. This assumption is based on the observation that film density scales with energy density [27,28]. Moreover, the phase shift between voltage and current was found to be  $-78^\circ$  in the web coater instead of  $-88^\circ$  for the batch reactor. Thus, the current density, which scales with electron density, is smaller within the larger reactor (for comparable  $W/F$  and  $V_0$ ) [29,30]. The possibility that the energy dissipated in the film (by ion bombardment) during growth is actually much lower in the web coater

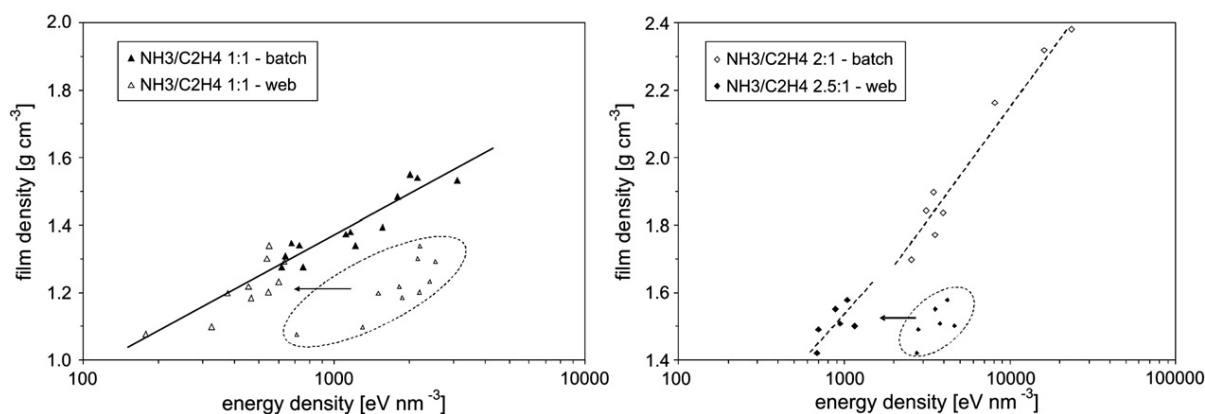


Fig. 4. Film density of a-C:H:N coatings as obtained for the two reactors depending on the energy density during film growth for  $\text{NH}_3/\text{C}_2\text{H}_4$  gas ratios of 1:1 (left) and 2:1/2.5:1 (right). The energy density in the web coater is adjusted to agree with the film density values for both reactors (see text).

compared to the batch reactor would also explain the obtained differences in the deposition rates for higher  $\text{NH}_3/\text{C}_2\text{H}_4$  gas ratios.

These observations show that beside the specific energy input into the gas phase, the energetic conditions (ions and fast neutrals impinging the surface) during film growth should also be considered for up-scaling plasma polymerization processes. Nevertheless, as long as the deposition follows an Arrhenius-like behavior (regime II), the film elemental composition (C, N, and O) is mainly determined by gas phase processes yielding the flux of film-forming species. For the web coater we obtained a-C:H:N coatings with a constant N concentration over the whole regime II ( $\text{N/C} = 0.24 \pm 0.02$  for  $\text{NH}_3/\text{C}_2\text{H}_4 = 1$ ). The deposited mass thus corresponds to the particle flux of the film-forming species originating from the active plasma zone (chemical reaction pathway). The amount of amino groups ( $-\text{NH}_2$ ), however, was found to decrease with increasing energy density, i.e. crosslinking (from 0.1 to 0.01 for  $\text{NH}_2/\text{C}$ ), which will be published in more detail elsewhere. Nitrogen-containing plasma polymer films can thus be optimized regarding their crosslinking (film density), deposition rate and functionality by using the presented macroscopic approach.

#### 4. Conclusions

$\text{NH}_3/\text{C}_2\text{H}_4$  discharges were investigated within a lab-scale and a pilot-scale reactor using a macroscopic approach regarding their deposition rates depending on power input and (monomer) flow rate. The reaction parameter  $W/F$  was found to support the transfer between the two reactors for the deposition of amine-functional plasma polymers. However, the film growth is also determined by the energy dissipated at its surface during the deposition given by ion flux times mean ion energy per deposition rate, which can be estimated for both reactors assuming that the film density scales with the energy density. Thus, lower plasma densities were found for the larger web coater, which might be caused by lower current densities, showing the importance of taking into account plasma geometry for up-scaling.

#### Acknowledgments

The authors like to acknowledge funding by the Swiss Commission of Technology and Innovation (CTI “FunkTex”) and the Swiss National Science Foundation (SNF “NanoTera”).

#### References

- [1] S. Guimond, B. Hanselmann, M. Amberg, D. Hegemann, *Pure Appl. Chem.* 82 (2010) 1239.
- [2] K.S. Siow, L. Britcher, S. Kumar, H.J. Griesser, *Plasma Processes Polym.* 3 (2006) 392.
- [3] S. Lischer, E. Körner, D.J. Balazs, D. Shen, P. Wick, K. Grieder, D. Haas, M. Heuberger, D. Hegemann, *J. R. Soc. Interface* (2011), doi:10.1098/rsif.2010.0596.
- [4] R. d'Agostino, et al., (Eds.), *Advanced Plasma Technology*, Wiley-VCH, Weinheim, 2008.
- [5] D.E. Robinson, D.J. Buttle, J.D. Whittle, K.L. Parry, R.D. Short, D.A. Steele, *Plasma Processes Polym.* 7 (2010) 102.
- [6] H.-E. Wagner, in: R. Hippler, et al., (Eds.), *Low Temperature Plasma Physics*, Wiley-VCH, Berlin, 2001, p. 305.
- [7] D. Hegemann, E. Körner, S. Guimond, *Plasma Processes Polym.* 6 (2009) 246.
- [8] D. Hegemann, E. Körner, S. Guimond, *Proc. 53rd SVC Ann. Technical Conf.* 2010, p. 23, Orlando/FL.
- [9] S.Y. Park, N. Kim, U.Y. Kim, S.I. Hong, H. Sasabe, *Polym. J.* 22 (1990) 242.
- [10] D. Hegemann, *Thin Solid Films* 515 (2006) 2173.
- [11] D. Hegemann, E. Körner, K. Albrecht, U. Schütz, S. Guimond, *Plasma Processes Polym.* 7 (2010) 889.
- [12] K.K. Gleason, *Plasma Processes Polym.* 7 (2010) 380.
- [13] S. Engelmann, R.L. Bruce, F. Weinboeck, G.S. Oehrlein, D. Nest, D.B. Graves, C. Andes, E.A. Hudson, *Plasma Processes Polym.* 6 (2009) 484.
- [14] M.A. Liebermann, A.J. Lichtenberg, *Principles of Plasma Discharges and Materials Processing*, 2nd ed. Wiley, Hoboken/NJ, 2005.
- [15] A. Manenschijn, W.J. Goedheer, *J. Appl. Phys.* 69 (1991) 2923.
- [16] E. Körner, G. Fortunato, D. Hegemann, *Plasma Processes Polym.* 6 (2009) 119.
- [17] M.M. Hossain, J. Müssig, A.S. Herrmann, D. Hegemann, *J. Appl. Polym. Sci.* 111 (2009) 2545.
- [18] M.M. Hossain, D. Hegemann, G. Fortunato, M. Heuberger, *Plasma Processes Polym.* 4 (2007) 471.
- [19] A. Brockhaus, G.F. Leu, V. Selenin, K. Tarnev, J. Engemann, *Plasma Sources Sci. Technol.* 15 (2006) 171.
- [20] P. Favia, M.V. Stendardo, R. d'Agostino, *Plasmas Polym.* 1 (1996) 91.
- [21] D. Hegemann, M.M. Hossain, *Plasma Processes Polym.* 2 (2005) 554.
- [22] M.M. Hossain, A.S. Herrmann, D. Hegemann, *Plasma Processes Polym.* 4 (2007) 135.
- [23] F. Truica-Marasescu, M.R. Wertheimer, *Plasma Processes Polym.* 5 (2008) 44.
- [24] J. Benedikt, *J. Phys. D Appl. Phys.* 43 (2010) 043001.
- [25] J.C. Ruiz, et al., *Plasma Process. Polym.* 7 (2010) 737.
- [26] D. Hegemann, M.M. Hossain, E. Körner, D.J. Balazs, *Plasma Processes Polym.* 4 (2007) 229.
- [27] M. Weiler, S. Sattel, T. Giessen, K. Jung, H. Ehrhardt, V.S. Veerasamy, J. Robertson, *Phys. Rev. B* 53 (1996) 1594.
- [28] S. Peter, K. Graupner, D. Grambole, F. Richter, *J. Appl. Phys.* 102 (2007) 053304.
- [29] A. von Engel, *Electric Plasmas: Their Nature and Uses*, Taylor & Francis, London, 1983.
- [30] G. Janzen, *Plasmatechnik*, Hüthig, Heidelberg, 1992.